Adaptive Force Control of Position/Velocity Controlled Robots: Theory and Experiment

Jaydeep Roy, *Member, IEEE*, and Louis L. Whitcomb, *Member, IEEE*

***Abstract*—This paper addresses the problem of achieving exact dynamic force control with manipulators possessing the low-level position and/or velocity controllers typically employed in industrial robot arms. Previously reported approaches and experimental results are reviewed. A new adaptive force control algorithm for velocity/position controlled robot arms in contact with surfaces of unknown linear compliance is reported. The controller provably guarantees global asymptotic convergence of force trajectory tracking errors to zero when the robot is under exact or asymptotically exact inner loop velocity control. An additional result which guarantees arbitrarily small force errors for bounded inner loop velocity tracking errors is presented. Comparative experiments show the new adaptive velocity (position) based controller and its nonadaptive counterpart to provide performance superior to that of previously reported position-based force controllers.**

***Index Terms*—Adaptive force control, implicit force control, position-based force control, robot force control, stability.**

I. Introduction

THIS PAPER addresses the problem of achieving exact dynamic force control with manipulators possessing the low-level position and/or velocity controllers typically employed in industrial robot arms. We report a new adaptive inner loop/outer loop force controller for one-dimensional (1-D) velocity/position controlled robot arms in contact with surfaces of unknown linear compliance. We present a proof of the global asymptotic stability of the adaptive controller as well as its nonadaptive counterpart for force trajectory tracking when the robot is under exact or asymptotically exact inner loop velocity control. To the best of our knowledge, this is the first reported proof of global asymptotic stability in force trajectory tracking for this class of position/velocity based force controllers. We report an additional high gain result which guarantees arbitrarily small force tracking errors with the controller for bounded inner loop velocity tracking errors. Finally, we present experimental data which: 1) corroborates the theoretical results presented in this paper and 2) shows the performance of the new adaptive force tracking controller and its nonadaptive counterpart to be superior to that of the position-based integral force controller. The remainder of the section briefly reviews existing force control literature and motivates our work.

The robot force control literature reports two broad approaches for the control of robots executing constrained motion: impedance control and hybrid (force/position) control [1]. In impedance control, a prescribed static or dynamic relation is sought to be maintained between the robot end effector force and position [2]–[4]. In hybrid control, the end effector force is explicitly controlled in selected directions and the end effector position is controlled in the remaining (complementary) directions [5], [6]. Reported hybrid control approaches can further be classified into three main categories: 1) explicit (model based) hybrid control of rigid robots in hard contact with a rigid environment, e.g., [5], [7], [8]; 2) explicit (model based) hybrid control of rigid robots in soft contact with a compliant environment, e.g., [9]–[11]; and 3) implicit (position/velocity based) hybrid control of rigid robots in soft contact with a compliant environment, e.g., [12]. In *explicit* hybrid control, the end-effector force is controlled by directly commanding the joint torques of the robot based on the sensed force error. Controllers based on this approach often employ the full rigid body dynamical model of the robot. In *implicit* hybrid control, the end-effector force is controlled indirectly by modifying the reference trajectory of an inner loop joint position/velocity controller based on the sensed force error. Controllers based on this approach usually do not require the rigid body dynamical model of the robot. Fig. 1 shows a schematic of the three approaches for the 1-D case. Note that, in one dimension, the hybrid control problem reduces to a pure force control problem. Other force control approaches which incorporate either fourth- or sixth-order dynamics in the contact model have been reported [13]–[15] but are not reviewed here.

The explicit hybrid control method was first proposed in [5] with the aim of implementing force control on torque-controlled robot arms (typically direct-drive arms). The controller guaranteed asymptotically exact force set-point regulation. A variety of explicit dynamic/model-based hybrid controllers which take into account the full rigid body dynamical model of the robot and guarantee asymptotically exact force trajectory tracking have since been proposed for the hard contact case, e.g., [7], [8]. Adaptive sliding mode hybrid controllers, which estimate the robot plant parameters online and guarantee asymptotically exact force trajectory tracking, have been reported, e.g., [16], [17]. Similarly, for the soft contact case, model-based adaptive and nonadaptive controllers which guarantee asymptotically exact force set-point regulation [9] and asymptotically exact force trajectory tracking [10] have been reported. Recently, a model-based hybrid controller that adaptively estimates the

Manuscript received January 10, 2001; revised October 22, 2001. This paper was recommended for publication by Associate Editor D. Pai and Editor I. Walker upon evaluation of the reviewers' comments. This work was supported in part by the National Science Foundation (NSF) under Grant BES-9625143. The robot employed in the experiments was developed under NSF Grant IIS9801684 and the Engineering Research Center Grant EEC9731478. This paper was presented in part at the IEEE/RSJ International Conference on Intelligent Robots and Systems, Maui, HI, November 2001.

The authors are with the Department of Mechanical Engineering, Johns Hopkins University, Baltimore, MD 21218 USA (e-mail: llw@jhu.edu).

Publisher Item Identifier S 1042-296X(02)02652-6.

1042-296X/02$17.00 © 2002 IEEE

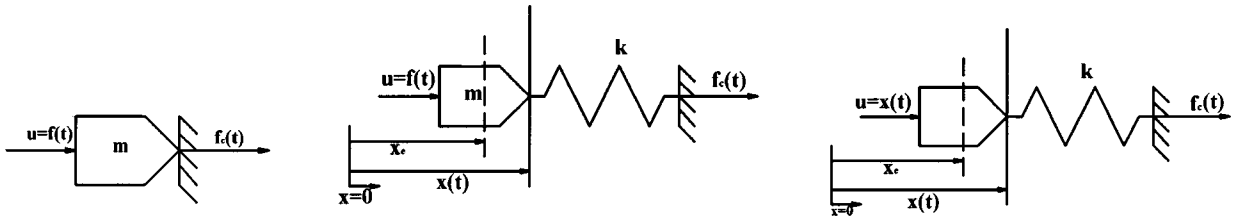

(a) (b) (c)

Fig. 1. Three reported approaches to robot force control. (a) Explicit (model-based) force control of robots in hard contact with a rigid environment. (b) Explicit (model-based) force control of robots in soft contact with a compliant environment. (c) Implicit (position/velocity) based force control of robots in soft contact with a compliant environment.

environment compliance and guarantees exponentially exact force trajectory tracking has been reported for the soft contact case [11]. The reader is referred to [1] for a more detailed survey of model-based impedance and hybrid force/position control results. Note that while these explicit model-based approaches can be directly applied to the force control of torque-controlled robot arms, they do not directly address the case of achieving force control with industrial arms possessing low-level position and/or velocity control.

The implicit hybrid control method, in which an outer force loop is closed around an inner position loop, was proposed in [12] with the aim of implementing force control on traditional industrial manipulators. Industrial manipulators have the following salient features.

1) The robot is position-controlled, i.e., the joint torques are commanded by a lower level position controller. User access to the joint torques and/or the lower level motion controller is typically restricted or not available—force or impedance control loops can only be closed around position/velocity control loops.
2) The joints have gearboxes (e.g., cycloidal, harmonic, ball screw), which typically have significant friction and are nonbackdrivable.
3) The complete rigid body dynamic model of the manipulator is generally not available or is not employed.

In [12], the authors presented an integral outer loop force control law (and a PI variant) which provides asymptotically exact force set point regulation in the absence of inner loop velocity tracking errors and bounded force errors in the presence of bounded inner loop velocity errors. Impedance control methods based on an inner position loops were presented in [18]–[20]. In [18], the authors also study the effect of unmodeled interaction forces on the inner position loop and show that bounded end-effector forces lead to (arbitrarily small) bounded position and velocity errors in the inner PD position control loop. Subsequently reported studies of implicit force and impedance control have focused on practical and implementation issues. In [21], an implicit hybrid controller in implemented for an automated deburring task in which the robot end-effector is made to follow a curved surface while applying a constant force normal to the surface. The effects of static friction on an implicit PI force controller are studied in [22]. Contact stability issues in a variant of the implicit PI hybrid controller and a new implicit impedance controller are theoretically and experimentally studied in [23], [24]. The effects of joint torsional elasticity on an implicit integral force controller and an implicit impedance controller are described in [25] and [26] respectively, while the interplay between the integrator in the inner PID loop and joint flexibility is studied in [27]. The development of a hydro-elastic actuator which implements an implicit PI type force controller is reported in [28].

While most previously reported implicit hybrid (or force) controllers guarantee asymptotically exact force set point regulation under exact inner loop position/velocity control, none provides asymptotically exact force trajectory tracking. To the best of our knowledge, no provably asymptotically stable implicit force trajectory tracking controller has been reported previously in literature. This paper attempts to fill this lacuna by presenting two new implicit force controllers which provably guarantee asymptotically exact force trajectory tracking under exact or asymptotically exact inner loop velocity control. Specifically, the objectives of this paper are threefold.

1) We report two new velocity based implicit force trajectory tracking controllers (one which requires knowledge of the environment compliance and another which adaptively determines the environment compliance) and present proofs of their global asymptotic stability. The controllers provably guarantee globally asymptotically exact force trajectory tracking under exact or asymptotically exact inner loop velocity tracking.
2) We prove that force trajectory tracking errors are bounded and can be made arbitrarily small in the presence of bounded inner loop velocity errors.
3) We report a comparative experimental investigation of the two new controllers and the popular implicit integral force set-point regulator over a wide range of reference force trajectories which shows the performance of the new controllers to be superior to that of the set-point regulator.

The rest of the paper is organized as follows. In Section II, we state the assumptions on the 1-D plant model and formulate the control problem. In Section III, we state and prove a useful lemma which is used in later stability proofs. In Section IV, we review one previously reported implicit controller and present two new implicit force controllers, and provide global stability proofs for the new controllers under the progressively weaker assumptions of exact inner loop velocity control, asymptotically exact inner loop velocity control and bounded inner loop velocity errors. In Section V, we present comparative experimental results which corroborate the theory and compare the performance of the new controllers with the previously reported set-point regulator. Section VI concludes and summarizes the results.

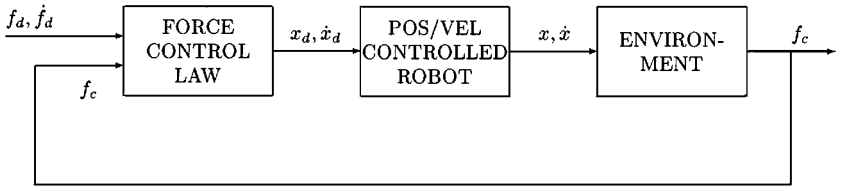

(a)

Symbol	Meaning	SI unit
$f_c(t)$	Contact force	N
$\dot{f}_c(t)$	First time derivative of contact force	N/s
$f_d(t)$	Desired force trajectory	N
$\dot{f}_d(t)$	First time derivative of desired force trajectory	N/s
$\Delta f = f_c(t) - f_d(t)$:	Force tracking error	N
$x(t)$	Actual position	m
$\dot{x}(t)$	Actual Velocity	m/s
$x_d(t)$	Desired position	m
$\dot{x}_d(t)$	Desired velocity	m/s
$\Delta x(t) = x(t) - x_d(t)$	Position tracking error	m
$\Delta \dot{x}(t) = \dot{x}(t) - \dot{x}_d(t)$	Velocity tracking error	m/s
x_e	Undeformed environment position (position corresponding to zero force)	m
k	Combined robot end-point, sensor and environment stiffness	N/m
$\gamma = 1/k$	Combined robot end point, sensor and environment compliance	m/N
$\hat{\gamma}(t)$	Time varying estimate of γ	m/N
$\dot{\hat{\gamma}}(t)$	First time derivative of $\hat{\gamma}$	m/ N-s
$\tilde{\gamma}(t) = \hat{\gamma}(t) - \gamma$	Error in the compliance estimate	m/N
$u(t, f_d, \dot{f}_d, \Delta f, \hat{\gamma})$	Outer loop force control law to be designed	m
$g(t, f_d, \dot{f}_d, \Delta f)$	Adaptive update law to be designed	m/N

(b)

Fig. 2. (a) Schematic block diagram of the plant, environment and controller. (b) Notation used.

II. Problem Statement: Force Control With 1-D Position/Velocity Control

Fig. 2(a) shows a schematic block diagram of the plant, environment, controller and the states, inputs, and outputs of the system for the 1-D problem while Fig. 2(b) defines the notation used in the block diagram and the rest of the paper. The entire inner loop system comprising of the mechanical robot and the position/velocity controller will henceforth be referred to as the robot plant or simply as the plant. Further, k and γ will be referred to simply as the environment stiffness and environment compliance, respectively.

A. Plant Model

The following assumptions are made regarding the 1-D robot plant.

1) The robot position $x(t)$ and velocity $\dot{x}(t)$ are the physical states of the plant and are continuous. The only input to the plant is the reference velocity trajectory $\dot{x}_d(t)$ and the outputs are the actual velocity $\dot{x}(t)$ and the actual position $x(t)$. The tracking error of the plant can be written as

$$\Delta \dot{x}(t) = \dot{x}(t) - \dot{x}_d(t). \tag{1}$$

2) The robot is always in soft bilateral contact with the environment and the environment compliance is linear. That is, both k and γ are nonzero finite positive numbers and the robot end-point contact force satisfies the following equation:

$$f_c(t) = k(x(t) - x_e). \tag{2}$$

Alternatively, we can write

$$x(t) = \gamma f_c(t) + x_e. \tag{3}$$

3) The robot position, velocity, and end point force are sensed and are available to the outer loop force controller.

B. Inner Loop Velocity Control: Assumptions

In addition to traditional proportional (P) and proportional-integral (PI) velocity control schemes (which guarantee bounded velocity errors for bounded C^1 velocity trajectories), a variety of model-based position/velocity controllers (e.g., [29], [30]) have been reported in robot position control literature. These controllers guarantee asymptotically exact position and velocity tracking for all C^2 position trajectories for noncontact motion of the robot. For example, the 1-D robot plant

$$\tau = m\ddot{x}(t), \tag{4}$$

under the velocity control law

$$\tau = m\ddot{x}_d(t) - k_d \Delta \dot{x}(t) \tag{5}$$

exhibits closed-loop dynamics given by

$$m\Delta \ddot{x}(t) + k_d \Delta \dot{x}(t) = 0. \tag{6}$$

For all C^1 desired velocity trajectories, $\dot{x}_d(t)$, the closed-loop system results in a bounded velocity error $\Delta \dot{x}(t)$ that satisfies

$$\lim_{t \to \infty} \Delta \dot{x}(t) = 0. \tag{7}$$

Note that (7) theoretically holds irrespective of whether the reference velocity, $\dot{x}_d(t)$, is bounded or unbounded. This is in contrast to P or PI velocity controllers, which guarantee bounded velocity errors *only if* the reference velocity trajectory, $\dot{x}_d(t)$, is bounded.

When a typical stiff industrial manipulator, under a "model-based" control law similar to (5), is in contact with with a significantly compliant environment, we can assume one of the following.

B1: The effect of the contact force on the inner velocity loop is negligible because of the nonbackdrivability of most industrial gear trains. Thus the velocity error asymptotically converges to zero.

B2: The environment is soft enough that the contact force acts as a bounded disturbance on the system. This results in a bounded steady-state velocity tracking error.

Note that assumptions (B1) and (B2) on the inner loop velocity tracking error hold for all (bounded as well as unbounded) C^1 reference velocity trajectories. The control task, then, is to design an outer loop force control law that results in a bounded reference velocity trajectory to the inner loop velocity controllers and provides asymptotically exact force trajectory tracking. Sections II-C and II-D formally state the control problem.

C. Control Task: Known Environment Compliance

Given the plant defined by (1)–(3), a known environment compliance γ and a bounded time-varying $\mathcal{C}^2$ reference force trajectory, $f_d(t)$, with bounded time derivatives, $\dot{f}_d(t)$ and $\ddot{f}_d(t)$, the control task is to choose an outer loop force control law of the form

$$\dot{x}_d(t) = u(t, f_d, \dot{f}_d, \Delta f) \tag{8}$$

such that $\Delta f(t)$ is bounded for all $t > 0$ and satisfies each of the following:

Case 1) **Exact inner loop velocity tracking:**

$$\lim_{t\to\infty} \Delta f(t) = 0 \quad \text{if} \quad \Delta\dot{x} = 0 \quad \forall t. \tag{9}$$

Case 2) **Asymptotically exact inner loop velocity tracking:**

$$\lim_{t\to\infty} \Delta f(t) = 0 \quad \text{if} \quad \lim_{t\to\infty} \Delta\dot{x} = 0. \tag{10}$$

Case 3) **Bounded inner loop steady-state velocity errors:**

$$\limsup_{t\to\infty} |\Delta f(t)| \le \beta \quad \text{if} \quad \limsup_{t\to\infty} |\Delta\dot{x}| \le M \tag{11}$$

where $0 \le M < \infty$ is a finite bound on the steady-state velocity error and β can be chosen to be an arbitrarily small positive number.

D. Control Task: Unknown Environment Compliance

For the case of an unknown linear environment compliance, given a bounded time-varying $\mathcal{C}^2$ reference force trajectory $f_d(t)$ with bounded time derivatives, $\dot{f}_d(t)$ and $\ddot{f}_d(t)$, the adaptive control problem is to choose an outer loop force control law of the form

$$\dot{x}_d(t) = u(t, f_d, \dot{f}_d, \Delta f, \hat{\gamma}) \tag{12}$$

and an adaptive update law of the form

$$\dot{\hat{\gamma}}(t) = g(t, f_d, \dot{f}_d, \Delta f) \tag{13}$$

such that $\hat{\gamma}(t)$ and $\Delta f(t)$ are bounded for all $t > 0$ and $\Delta f(t)$ satisfies each of the following:

Case 1) **Exact inner loop velocity tracking:**

$$\lim_{t\to\infty} \Delta f(t) = 0 \quad \text{if} \quad \Delta\dot{x} = 0 \,\forall t. \tag{14}$$

Case 2) **Asymptotically exact inner loop velocity tracking:**

$$\lim_{t\to\infty} \Delta f(t) = 0 \quad \text{if} \quad \Delta\dot{x}(t) \in \mathcal{L}_2 \quad \text{and} \quad \lim_{t\to\infty} \Delta\dot{x} = 0. \tag{15}$$

Case 3) **Bounded inner loop steady state velocity errors:**

$$\limsup_{t\to\infty} |\Delta f(t)| \le \beta \quad \text{if} \quad \limsup_{t\to\infty} |\Delta\dot{x}| \le M \tag{16}$$

where $0 \le M < \infty$ is a finite bound on the steady-state velocity error and β can be chosen to be an arbitrarily small positive number.

Note that, for the case of asymptotic inner loop velocity tracking, we require an additional assumption that $\Delta\dot{x}(t) \in \mathcal{L}_2$. We do not lose significant generality by making this additional restriction since most velocity controllers which guarantee asymptotically exact velocity tracking also guarantee that the velocity error is $\mathcal{L}_2$, e.g., [29], [30].

III. A Useful Lemma

In this section, we state and prove a lemma that will be used later in the paper. We note that the result presented in the lemma is a minor generalization of the well-known result from systems theory that the state of an asymptotically stable LTI system asymptotically decays to zero when driven by an input which asymptotically decays to zero. The proof of the lemma is very similar to the proof of the above result but is included here for clarity and completeness.

Lemma III.1: Given real numbers $0 < a < \infty$ and $0 \le M < \infty$ and a real valued continuous function $\psi(t) : [0, \infty) \to R$ which has the property

$$\limsup_{t\to\infty} |\psi(t)| \le M \tag{17}$$

the convolution of $\psi(t)$ with e^{-at} satisfies the following inequality:

$$\limsup_{t\to\infty} \left| \int_0^t e^{-a(t-\tau)} \psi(\tau)\, d\tau \right| \le \frac{1}{a} M. \tag{18}$$

Proof: Continuity of $\psi(t)$ and (17) implies $\psi(t)$ is bounded $\forall t$. Further, property (17) ensures that, given any $\epsilon > 0$, there exists a $T > 0$ such that

$$|\psi(t)| \le M + \epsilon \quad \forall t > T. \tag{19}$$

Using the triangle inequality, $\forall t > T$, we obtain

$$\left|\int_0^t e^{-a(t-\tau)}\psi(\tau)\,d\tau\right| \leq \left|\int_0^T e^{-a(t-\tau)}\psi(\tau)\,d\tau\right| + \left|\int_T^t e^{-a(t-\tau)}\psi(\tau)\,d\tau\right| \quad (20)$$

$$\leq e^{-at}\left|\int_0^T e^{a\tau}\psi(\tau)\,d\tau\right| + \int_T^t e^{-a(t-\tau)}|\psi(\tau)|\,d\tau \quad (21)$$

$$\leq e^{-at}\left|\int_0^T e^{a\tau}\psi(\tau)\,d\tau\right| + (M+\epsilon)\int_T^t e^{-a(t-\tau)}\,d\tau \quad (22)$$

where we have used property (19) in concluding (22) from (21). Taking limits of both sides as $t \to \infty$ gives

$$\limsup_{t\to\infty}\left|\int_0^t e^{-a(t-\tau)}\psi(\tau)\,d\tau\right| \leq \lim_{t\to\infty}(M+\epsilon)\left[\int_T^t e^{-a(t-\tau)}\,d\tau\right]. \quad (23)$$

Evaluating the integral on the right-hand side gives

$$\limsup_{t\to\infty}\left|\int_0^t e^{-a(t-\tau)}\psi(\tau)\,d\tau\right| \leq \lim_{t\to\infty}(M+\epsilon)\frac{1}{a}[1-e^{-a(t-T)}]. \quad (24)$$

Finally, noting that T is fixed and finite for any given ϵ and evaluating the limit on the right-hand side of the inequality gives

$$\limsup_{t\to\infty}\left|\int_0^t e^{-a(t-\tau)}\psi(\tau)\,d\tau\right| \leq \frac{1}{a}(M+\epsilon). \quad (25)$$

Since (25) holds for all positive values of ϵ, we obtain

$$\limsup_{t\to\infty}\left|\int_0^t e^{-a(t-\tau)}\psi(\tau)\,d\tau\right| \leq \frac{1}{a}M. \quad (26)$$

■

IV. Three Force Control Algorithms: The 1-D Case

In this section, we review one reported implicit force controller and present two new velocity-based implicit force controllers and give mathematical proofs that these controllers are stable and perform the control tasks described in (9)–(11).

A. Implicit Force Set Point Regulator

The implicit set point regulator (SPR) was proposed in [12]. The authors proposed the following outer loop integral force control law:[1]

$$x_d(t) = -k_f\int_0^t \Delta f(\tau)\,d\tau, \quad k_f > 0. \quad (27)$$

In terms of reference velocity, the control law can be restated as

$$\dot{x}_d(t) = -k_f\Delta f(t). \quad (28)$$

[1]The actual force control law proposed was $x_d(t) = k^{-1}k_f\int_0^t \Delta f(\tau)\,d\tau$. Since k^{-1} adds nothing to the analysis we present and can be incorporated in k_f, we ignore the term in our review

Since then, several variants of this law have been proposed (see the review in Section I). For a *constant* desired force f_d, the closed-loop equation of plant (1), (2), and (3) under control law (28) can be written as

$$\Delta\dot{f}(t) + kk_f\Delta f(t) = k\Delta\dot{x}(t). \quad (29)$$

For a constant desired force f_d, the controller (28) guarantees asymptotically exact force regulation when the inner loop velocity controller provides exact or asymptotically exact velocity tracking. In the case of bounded steady-state inner loop velocity errors, it can be shown that the force tracking errors satisfy

$$\limsup_{t\to\infty}|\Delta f(t)| \leq \frac{1}{k_f}M \quad \text{if} \quad \limsup_{t\to\infty}|\Delta\dot{x}(t)| \leq M \quad (30)$$

where $\Delta\dot{x}(t)$ and $\Delta f(t)$ denote the velocity and force errors, respectively.

The case of following a *time-varying* reference force trajectory is not addressed in [12]. We note here that even in the case of exact inner loop velocity tracking, the controller (28) does not guarantee asymptotically exact force trajectory tracking. In [12], the authors also propose a PI variant

$$x_d(t) = -k_{fp}\Delta f(t) - k_{fi}\int_0^t \Delta f(\tau)\,d\tau \quad (31)$$

of the control law (27). However, we note that (31) does not provide asymptotically exact force trajectory tracking even in the presence of exact inner loop velocity tracking. Since for the case of force set point regulation, the closed-loop equation arising from control law (31) is identical to the closed-loop equation (29) of control law (27), with $k_f = k_{fi}/k_{fp}$, we do not pursue a separate analysis of this control law herein.

B. Implicit Force Trajectory Tracking Controller

In this section, we propose a force trajectory tracking control (TTC) law for the case where the environment compliance γ is known *a priori*. The control law is based on the implicit force SPR law reviewed in Section IV-A, augmented by a term that feeds forward an estimate of the desired velocity for the inner loop controller. Specifically, for the task of following a bounded time-varying $\mathcal{C}^2$ force reference $f_d(t)$, with bounded first time derivatives, $\dot{f}_d(t)$ and $\ddot{f}_d(t)$, we propose the following outer loop force control law:

$$\dot{x}_d(t) = \gamma\dot{f}_d(t) - k_f\Delta f(t) \quad (32)$$

where $k_f > 0$ is the force gain. To the best of our knowledge, this controller has not been previously reported in literature. Observe that control law (32) is identical to the SPR of Section IV-A for the special case of a *constant* desired force f_d.

We now show that the plant (1) under the outer loop force control law (32) is globally asymptotically stable in force trajectory tracking errors when the robot is under exact and asymptotically exact inner loop velocity control and that the force trajectory tracking errors can be made arbitrarily small when there are bounded inner loop velocity tracking errors.

Theorem IV-B.1: For any bounded C^2 reference force trajectory $f_d(t)$, with bounded time derivatives, $\dot{f}_d(t)$ and $\ddot{f}_d(t)$, the control law

$$\dot{x}_d(t) = \gamma \dot{f}_d(t) - k_f \Delta f(t), \quad k_f > 0 \tag{33}$$

acting on the plant

$$\dot{x}(t) = \dot{x}_d(t) + \Delta \dot{x}(t) \tag{34}$$

$$f_c(t) = k(x(t) - x_e) \tag{35}$$

guarantees bounded force tracking error $\Delta f(t)$. Further, $\Delta f(t)$ satisfies

$$\lim_{t\to\infty} \Delta f(t) = 0 \quad \text{if} \quad \Delta \dot{x} = 0 \quad \forall t; \tag{36}$$

$$\lim_{t\to\infty} \Delta f(t) = 0 \quad \text{if} \quad \lim_{t\to\infty} \Delta \dot{x} = 0; \tag{37}$$

$$\limsup_{t\to\infty} |\Delta f(t)| \le \frac{1}{k_f} M \quad \text{if} \quad \limsup_{t\to\infty} |\Delta \dot{x}| \le M \tag{38}$$

where $0 \le M < \infty$.

Proof: Substituting from (33) into the plant model (34), we get

$$\dot{x}(t) = \gamma \dot{f}_d(t) - k_f \Delta f(t) + \Delta \dot{x}. \tag{39}$$

Multiplying (39) by the environment stiffness $k(=1/\gamma)$, and rearranging terms, we get

$$k\dot{x}(t) - \dot{f}_d(t) + k k_f \Delta f(t) = k \Delta \dot{x}(t). \tag{40}$$

Finally, noting that $\dot{f}_c(t) = k\dot{x}(t)$ and that

$$\Delta \dot{f}(t) = \dot{f}_c(t) - \dot{f}_d(t) = \frac{d}{dt} \Delta f(t)$$

we can write the equation of the closed-loop system as

$$\Delta \dot{f}(t) + k k_f \Delta f(t) = k \Delta \dot{x}(t). \tag{41}$$

With this analysis, the closed-loop system (41) is a first-order time-invariant linear system driven by a bounded input $k\Delta\dot{x}(t)$. Since $k_f > 0$, the unforced linear system

$$\Delta \dot{f}(t) + k k_f \Delta f(t) = 0 \tag{42}$$

is exponentially stable. Hence the forced linear system (41) is bounded-input bounded-output stable [31]. Thus, for any bounded initial error $\Delta f(0)$, the force tracking error $\Delta f(t)$ is bounded.

Next define

$$\psi(t) = k \Delta \dot{x}(t). \tag{43}$$

Then the closed-loop system (41) has the solution

$$\Delta f(t) = \Delta f(0) e^{-k k_f t} + \int_0^t e^{-k k_f (t-\tau)} \psi(\tau)\, d\tau \tag{44}$$

where $\Delta f(0)$ is the bounded initial force error. Since $k_f > 0$, we obtain

$$\limsup_{t\to\infty} |\Delta f(t)| \le \limsup_{t\to\infty} \left| \int_0^t e^{-k k_f (t-\tau)} \psi(\tau)\, d\tau \right|. \tag{45}$$

Case 1) **Exact inner loop velocity tracking:**
Note that

$$\Delta \dot{x}(t) = 0 \quad \forall t \Rightarrow \psi(t) = 0 \quad \forall t.$$

Thus, from (45), we obtain

$$\lim_{t\to\infty} \Delta f(t) = 0. \tag{46}$$

Case 2) **Asymptotically exact inner loop velocity tracking:**
Note that

$$\lim_{t\to\infty} \Delta \dot{x}(t) \Rightarrow \lim_{t\to\infty} \psi(t) = 0. \tag{47}$$

Thus, given any $\epsilon > 0$, there exists a $T > 0$ such that

$$|\psi(t)| \le \epsilon \quad \forall t > T. \tag{48}$$

From (48), (45), and Lemma III.1, we obtain

$$\limsup_{t\to\infty} |\Delta f(t)| \le \frac{1}{k k_f} \epsilon. \tag{49}$$

Since (49) holds for all positive ϵ, however small, in the limit, we obtain

$$\lim_{t\to\infty} \Delta f(t) = 0. \tag{50}$$

Case 3) **Bounded inner loop steady-state velocity errors:**
Note that

$$\limsup_{t\to\infty} |\Delta \dot{x}(t)| \le M \Rightarrow \limsup_{t\to\infty} |\psi(t)| \le kM. \tag{51}$$

From (51), (45), and Lemma III.1, we get

$$\limsup_{t\to\infty} |\Delta f(t)| \le \frac{1}{k_f} M. \tag{52}$$

Thus, from (52), we see that in the presence of bounded steady-state inner loop velocity errors, the steady-state force tracking error $\Delta f(t)$ is bounded and can be made arbitrarily small by choosing a sufficiently large k_f. ■

1) Some Comments on Stability: A comment about the proof of Theorem IV-B.1 is appropriate here. We used the boundedness of $\Delta\dot{x}(t)$ in the closed-loop system (41) to conclude that the force error $\Delta f(t)$ is bounded. The boundedness of $\Delta f(t)$ and $\dot{f}_d(t)$ implies that the reference trajectory $\dot{x}_d(t)$, given by (32), to the inner loop velocity controller remains bounded for all time t. This, together with the boundedness of the desired force trajectory $f_d(t)$, guarantees that the states $\dot{x}(t)$ and $x(t)$ of the robot plant remain bounded under the outer loop control law (32).

While this argument proves the stability of the implicit force trajectory tracking controller when the robot is under model based inner-loop velocity control similar to that described in Section II-B (that is, inner loop control that theoretically guarantees bounded inner loop velocity errors for both bounded and unbounded velocity reference trajectories), it does not prove the stability of implicit force trajectory tracking when the robot is under traditional P or PI inner-loop velocity control. This is so because both the P and PI velocity controllers require that

velocity references be bounded in order to provide bounded velocity tracking errors. Once the boundedness of the inner loop velocity reference, $\dot{x}_d(t)$, is independently established, the boundedness of the velocity error $\Delta\dot{x}_d(t)$ immediately follows. The arguments in the proof of Theorem IV-B.1 then show that result (52) holds.

For inner loop P velocity control, we now proceed to show that the inner-loop velocity reference remains bounded under the outer-loop force control law (32). The 1-D plant

$$\tau(t) = m\ddot{x}(t) \tag{53}$$

under an inner loop P velocity control law

$$\tau(t) = -k_d\Delta\dot{x} \tag{54}$$

exhibits the closed-loop dynamics

$$m\ddot{x}(t) + k_d\Delta\dot{x}(t) = 0. \tag{55}$$

Noting that

$$\dot{x}(t) = \gamma\dot{f}_c(t) \quad \text{and} \quad \ddot{x}(t) = \gamma\ddot{f}_c(t) \tag{56}$$

and using (32), we obtain

$$m\gamma\ddot{f}_c(t) + k_d\{\gamma\dot{f}_c(t) - \gamma\dot{f}_d(t) + k_f\Delta f(t)\} = 0 \tag{57}$$

which implies that

$$m\Delta\ddot{f}(t) + k_d\Delta\dot{f}(t) + k_dk_f\Delta f(t) = -m\ddot{f}_d(t). \tag{58}$$

Since (58) is a time-invariant second-order asymptotically stable linear system driven by a bounded input $-m\ddot{f}_d(t)$, the states $\Delta f(t)$ and $\Delta\dot{f}(t)$ of the system are bounded for all positive force gains k_f. Hence, from (32), the reference velocity to the inner loop P velocity controller is bounded. Thus, the velocity error $\Delta\dot{x}(t)$ is bounded and result (52) follows.

For inner loop PI velocity control, an argument similar to that in (53)–(58) results in a third-order linear system with constant positive coefficients driven by a bounded input. As is well known, for a third-order system, there is a range of positive gains k_f for which the system is bounded-input bounded-output stable [31]. For this range of gains, result (52) holds and the force tracking error, $\Delta f(t)$, remains bounded. However, we note that it is always possible to choose a gain k_f which drives this closed-loop system into instability.

C. Implicit Adaptive Force Trajectory Tracking Controller (TTCA)

In this section, we report a new force trajectory tracking control law for the case where the environment compliance γ is not known. The control law is based on the implicit force trajectory tracking control law of Section IV-B. The only difference is that the feedforward term for the desired inner-loop velocity now uses an online estimate for environment compliance, which is determined by the adaptive update law. Specifically, for the task of following a bounded time-varying $\mathcal{C}^2$ force reference $f_d(t)$, with bounded time derivatives $\dot{f}_d(t)$ and $\ddot{f}_d(t)$, we propose the following outer loop force control law:

$$\dot{x}_d(t) = \hat{\gamma}(t)\dot{f}_d(t) - k_f\Delta f(t) \tag{59}$$

and the adaptive update law

$$\dot{\hat{\gamma}}(t) = -\alpha\dot{f}_d(t)\Delta f(t). \tag{60}$$

Here $\hat{\gamma}(t)$ is the time-varying estimate of the environment compliance, $k_f > 0$ is the force gain, and $\alpha > 0$ is the adaptive gain. To the best of our knowledge, this controller has not been previously reported in literature. Observe that control law (59) is identical to the set point regulator of Section IV-A for the special case of a *constant* desired force f_d.

We now show that the plant (1) under the outer loop force control law (59) and the update law (60) is globally asymptotically stable in force trajectory tracking errors when the robot is under exact and asymptotically exact inner loop velocity control.

Theorem IV-C.1: For any bounded $\mathcal{C}^2$ reference force trajectory $f_d(t)$, with bounded time derivatives, $\dot{f}_d(t)$ and $\ddot{f}_d(t)$, the control law

$$\dot{x}_d(t) = \hat{\gamma}(t)\dot{f}_d(t) - k_f\Delta f(t), \quad k_f > 0 \tag{61}$$

and the adaptive update law

$$\dot{\hat{\gamma}}(t) = -\alpha\dot{f}_d(t)\Delta f(t), \quad \alpha > 0 \tag{62}$$

acting on the plant

$$\dot{x}(t) = \dot{x}_d(t) + \Delta\dot{x}(t) \tag{63}$$

$$f_c(t) = k(x(t) - x_e) \tag{64}$$

guarantee bounded force tracking error $\Delta f(t)$ and bounded compliance estimate $\hat{\gamma}(t)$. Further, $\Delta f(t)$ satisfies

$$\lim_{t\to\infty}\Delta f(t) = 0 \quad \text{if} \quad \Delta\dot{x} = 0 \quad \forall t \tag{65}$$

$$\lim_{t\to\infty}\Delta f(t) = 0 \quad \text{if} \quad \Delta\dot{x}(t) \in \mathcal{L}_2 \quad \text{and} \quad \lim_{t\to\infty}\Delta\dot{x} = 0. \tag{66}$$

Proof: Substituting from (61) into the plant model (63), we obtain

$$\dot{x}(t) = \hat{\gamma}(t)\dot{f}_d(t) - k_f\Delta f(t) + \Delta\dot{x}. \tag{67}$$

Multiplying (67) by the environment stiffness $k(=1/\gamma)$, and rearranging terms, we obtain

$$k\dot{x}(t) - \dot{f}_d(t) + kk_f\Delta f(t) = k\tilde{\gamma}(t)\dot{f}_d(t) + k\Delta\dot{x}(t) \tag{68}$$

where $\tilde{\gamma}(t) = \hat{\gamma}(t) - \gamma$ is the error in the compliance estimate. Finally, noting that $\dot{f}_c(t) = k\dot{x}(t)$ and that

$$\Delta\dot{f}(t) = \dot{f}_c(t) - \dot{f}_d(t) = \frac{d}{dt}\Delta f(t)$$

we can write the equation of the closed-loop system as

$$\Delta\dot{f}(t) + kk_f\Delta f(t) = k\tilde{\gamma}(t)\dot{f}_d(t) + k\Delta\dot{x}(t). \tag{69}$$

Define

$$\psi(t) = k\Delta\dot{x}(t) \tag{70}$$

and note that

$$\Delta\dot{x}(t) = 0 \quad \forall t \Rightarrow \psi(t) = 0 \quad \forall t \tag{71}$$

$$\Delta\dot{x}(t) \in \mathcal{L}_2, \quad \lim_{t\to\infty}\Delta\dot{x}(t) = 0 \Rightarrow \psi(t) \in \mathcal{L}_2, \lim_{t\to\infty}\psi(t) = 0. \tag{72}$$

Since $\psi(t) \in \mathcal{L}_2$, there exists a number $0 \leq M < \infty$ such that

$$\int_0^t \psi(\tau)^2 \, d\tau \leq 4kk_f M \quad \forall t \in [0, \infty) \tag{73}$$

and observe that $M = 0$ if (71) holds. Define

$$V(t, \Delta f, \tilde{\gamma}) = \frac{1}{2}\Delta f(t)^2 + \frac{1}{2\alpha}k\tilde{\gamma}(t)^2 + M - \frac{1}{4kk_f}\int_0^t \psi(\tau)^2 d\tau \tag{74}$$

and note that (73) and (74) imply that $V(t, \Delta f, \tilde{\gamma}) \geq 0$ for all time t and that $V(t, \Delta f, \tilde{\gamma})$ is radially unbounded in Δf and $\tilde{\gamma}$. Observe that $V(t, \Delta f, \tilde{\gamma})$ is not a conventional Lyapunov function candidate since $V(t, 0, 0) = M$ and M may not equal 0 (as is required for Lyapunov function candidates [32]).
Differentiating (74) along the trajectories of the closed-loop system (69) and using (70), we obtain

$$\begin{aligned}
\dot{V}(t, \Delta f, \tilde{\gamma}) &= \Delta f(t)\Delta\dot{f}(t) + \frac{k}{\alpha}\tilde{\gamma}(t)\dot{\tilde{\gamma}}(t) - \frac{1}{4kk_f}\psi(t)^2 \\
&= \Delta f(t)\{-kk_f\Delta f(t) + k\tilde{\gamma}(t)\dot{f}_d(t) + \psi(t)\} \\
&\quad + \frac{k}{\alpha}\tilde{\gamma}(t)\dot{\tilde{\gamma}}(t) - \frac{1}{4kk_f}\psi(t)^2 \\
&= \left\{-kk_f\Delta f(t)^2 + \Delta f(t)\psi(t) - \frac{1}{4kk_f}\psi(t)^2\right\} \\
&\quad + \left\{k\tilde{\gamma}(t)\dot{f}_d(t)\Delta f(t) + \frac{k}{\alpha}\tilde{\gamma}(t)\dot{\tilde{\gamma}}(t)\right\}.
\end{aligned} \tag{75}$$

Noting that $\dot{\tilde{\gamma}}(t) = \dot{\hat{\gamma}}(t)$ and using (62), we obtain

$$\dot{V}(t, \Delta f(t), \tilde{\gamma}) = -\left\{\sqrt{kk_f}\Delta f(t) - \frac{1}{2\sqrt{kk_f}}\psi(t)\right\}^2. \tag{76}$$

Thus, $\dot{V}(t, \Delta f(t)\tilde{\gamma}) \leq 0 \quad \forall t$. Since $V(t, \Delta f, \tilde{\gamma}) \geq 0 \quad \forall t$, (74) and (76) imply that $\Delta f(t)$ and $\tilde{\gamma}(t)$ (and hence $\hat{\gamma}(t)$) are bounded and that

$$\begin{aligned}
\int_0^\infty \left\{\sqrt{kk_f}\Delta f(t) - \frac{1}{2\sqrt{kk_f}}\psi(t)\right\}^2 dt \\
\leq V(0, \Delta f(0), \tilde{\gamma}(0)) < \infty.
\end{aligned} \tag{77}$$

That is,

$$\left\{\sqrt{kk_f}\Delta f(t) - \frac{1}{2\sqrt{kk_f}}\psi(t)\right\} \in \mathcal{L}_2. \tag{78}$$

When either (71) or (72) holds, we have

$$\frac{1}{2\sqrt{kk_f}}\psi(t) \in \mathcal{L}_2. \tag{79}$$

From (78) and (79), using Minkowski's theorem [33], we obtain

$$\begin{aligned}
\sqrt{kk_f}\Delta f(t) = \left(\sqrt{kk_f}\Delta f(t) - \frac{1}{2\sqrt{kk_f}}\psi(t)\right) \\
+ \left(\frac{1}{2\sqrt{kk_f}}\psi(t)\right) \in \mathcal{L}_2.
\end{aligned} \tag{80}$$

Next, from (69), we see that $\Delta\dot{f}(t)$ is bounded and hence $\Delta f(t)$ is uniformly continuous. Hence, by Barbalat's Lemma [32], we obtain

$$\lim_{t\to\infty} \Delta f(t) = 0. \tag{81}$$

Thus, the adaptive controller (61) and (62) provides globally asymptotically exact force trajectory tracking when the plant (63) and (64) is under exact or asymptotically exact inner loop velocity control. ■

Two comments about Theorem IV-C.1 are appropriate here. First, we have only used the fact that the inner loop velocity error is $\mathcal{L}_2$ to prove that the force tracking error asymptotically converges to zero. Though we have not explicitly used that fact that the velocity error asymptotically converges to zero, we note that a $\mathcal{L}_2$ velocity error will not asymptotically converge to zero only if this error is not uniformly continuous [32]. However, since most reported position/velocity controllers that guarantee asymptotically exact velocity tracking also guarantee bounded acceleration errors (and hence uniformly continuous velocity errors), the slightly more general theoretical result that we have proved offers little practical advantage at the cost of obfuscating the utility of the result. Hence we make the stronger assumption that the inner velocity error is $\mathcal{L}_2$ *and* asymptotically converges to zero in the statement of Theorem IV-C.1. Second, a general high gain result which shows arbitrarily small asymptotic force tracking errors for asymptotically bounded inner loop velocity errors is currently not available. We note that *if* the compliance estimate error $\tilde{\gamma}$ is asymptotically bounded (by $M_1 \geq 0$ say), and $M_2 \geq 0$ is the bound on $\dot{f}d$, then (69) and Lemma III.1 show that

$$\limsup_{t\to\infty} \Delta f(t) \leq \frac{1}{k_f}(M_1 M_2 + M) \tag{82}$$

where M is the asymptotic bound on the velocity error. A theoretical result that enumerates the conditions under which the compliance estimate remains bounded in the presence of bounded inner loop velocity errors is currently not available. However, experimental results reported in Section V do show that in the presence of bounded inner loop velocity errors, the force errors remain bounded and can be made very small for a large range of input force trajectories, provided a large enough force gain k_f is chosen. This theoretically unexplained fact requires careful future attention.

V. Experimental Results

In this section, we report the results of comparative experiments using the three force control algorithms described in Section IV.

A. Experimental Setup

The arm used for these experiments was a seven degree of freedom robot arm developed at the Johns Hopkins University for medical applications [34], [35]. The arm has a three-degree-of-freedom linear base stage, a two-degree-of-freedom intermediate RCM stage [36], and a final two-degree-of-freedom $z - \theta$ stage. For the experiments reported in this section, all the joints of the arm, except one degree of freedom of the base stage, were immobilized. The active linear joint is actuated by a 24-V brushed dc motor (Pittman Model 14204C347) driven by a linear amplifier (Western Servo Design Model LDU-S1). The joint has a total gear reduction of 1000 π meters per radian. The joint was equipped with an encoder having a resolution of 4000

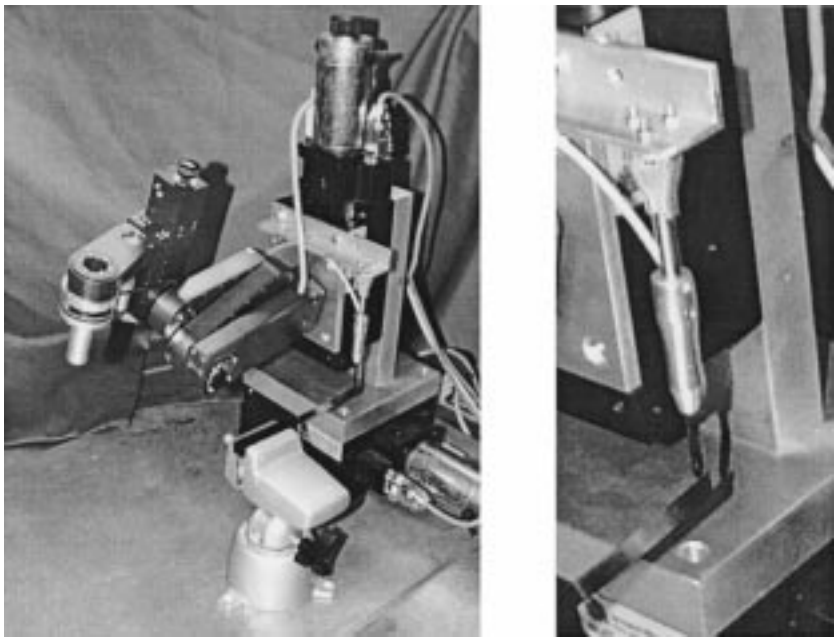

(a) (b)

Fig. 3. Experimental setup. Shown in the picture are the JHU steady hand robot, force sensor, and environment used in the experiments. For the experiments reported in this paper, all the joints of the arm, except one degree of freedom of the base stage, are immobilized. (a) Complete experimental setup. (b) Force sensor and environment.

counts per revolution resulting in a linear position resolution of 0.5 μm per encoder count.

The arm was equipped with a custom built single-axis tip force sensor which also served as the tool in the experiments. The force sensor has a maximum rating of ± 2 N and was sampled to an accuracy of 16 b for a force resolution of 6.4×10^{-5} N (64 μN). The ambient noise in the force sensor readings was of the order of 0.1 mN, leading to a force sensor accuracy of ± 0.1 mN.

The environment was thin spring steel beam rigidly fixed (cantilevered) at one end with the other end free. For small displacements of the free end, this beam approximates an environment with linear compliance. Fig. 3 shows the arm, the force sensor, and environment used in the experiments.

To accurately emulate an industrial situation, we implemented a simple proportional velocity controller on the active axis. This controller guarantees asymptotically exact velocity SPR (in the absence of coulomb friction) and bounded velocity errors for time-varying velocity reference trajectories. Except where explicitly noted, we used a velocity feedback gain, k_v, of 30 000 Ns/m for all the experiments reported in this section. We note here that one could alternatively implement a full-fledged model-based position/velocity inner loop controller which would guarantee asymptotically exact velocity trajectory tracking. However, since our goal was to independently verify each of the results reported in Section IV, including those for force tracking in the presence of bounded inner loop velocity errors, this asymptotically exact inner loop controller was not implemented.

It is well known that, for a given reference trajectory and a given controller, the force (and other state) errors can be made selectively small by increasing the feedback gains as high as possible (to the verge of instability). Further, high gains which lead to small errors for any one given reference trajectory and controller may lead to instability for another combination of reference trajectory and controller. Since we are primarily interested in *comparing* the *relative* performance of different controllers in an unbiased fashion over a wide range of reference trajectories, we did not push gains to the verge of instability to obtain the smallest tracking error magnitude for each reference trajectory and controller pair. Higher feedback gains were observed (off-course) to provide proportionally lower steady-state tracking errors but the relative performance of the various controllers remained unchanged. Except where explicitly noted otherwise, the feedback force gain of $k_f = 0.5$ m/Ns was uniformly employed for all controllers and all reference trajectories. Further, except where noted, the adaptive gain α of the TTCA controller is chosen to be 1.0 m/N^3 for all reference trajectories.

B. Force Set Point Regulation

All the three implicit force controllers presented in Section IV are identical for the problem of force set point regulation. Fig. 4 shows the reference and actual force trajectories when the robot is commanded to follow a step force input of 0.5 N for various different force feedback gain values, k_f. As predicted by theory, the robot displays a linear first-order exponential response with the response times decreasing with increasing force gains. The steady-state errors are a manifestation of the unmodeled friction and stiction terms in the inner loop velocity controller. However, again as predicted by the theory, both the inner loop velocity errors as well as the effect of the velocity errors on the force error decrease with increasing values of k_f and can be made very small (less than 0.3% for $k_f = 0.5$). Note that the initial small oscillations in the force response seen for the high force gain value of $k_f = 0.5$ (which is the only deviation from

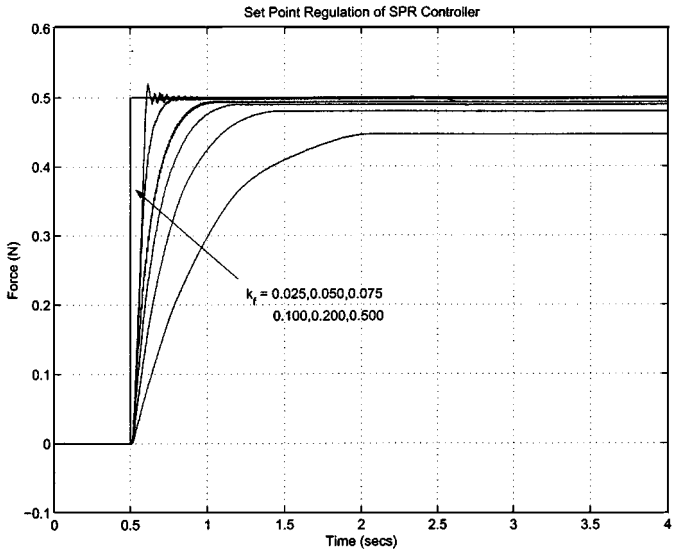

Fig. 4. Force set point regulation: Force response of implicit force controllers for a step force input of 0.5 N. Shown are the responses at $k_f = 0.025, 0.050, 0.075, 0.100, 0.200, 0.500$.

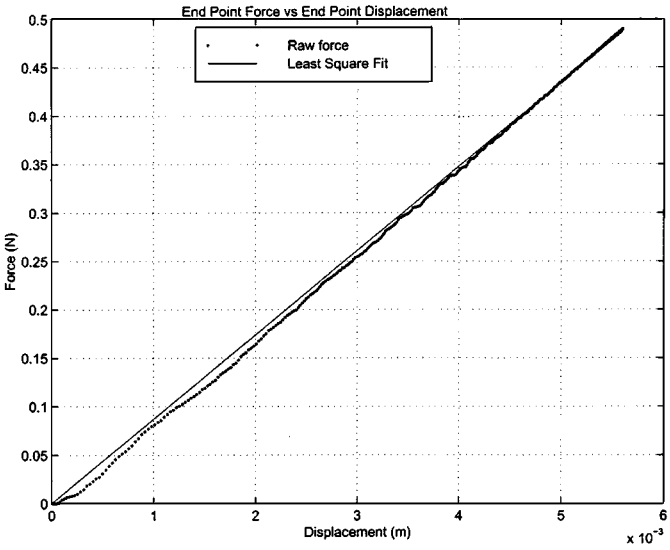

Fig. 5. Robot end point force versus displacement. The slope of the best fit line gives $k = 86.9$ N/m and $\gamma = 0.0115$ m/N.

theory observed in this set of experiments) are an artifact of the motor reaching its torque-velocity saturation limit. Finally, Fig. 5 shows the relationship between the tip forces and displacement for one of the above experiments. From the figure, we see that the net tool and environment compliance is linear. A best fit curve gives the value of the compliance, γ to be 0.0115 m/N.

C. Force Trajectory Tracking: Comparative Results

To evaluate the force trajectory tracking performance of controllers presented in Section IV, each of the three controllers (SPR, TTC, and TTCA) was made to ten different smooth force trajectories of the form

$$f_d(t) = 0.3 + 0.2\sin(2\pi f t) \quad \text{N} \tag{83}$$

where the frequency f of the reference sinusoid varied from 0.25 to 3.0 Hz in the different experiments. Fig. 6 shows the reference and the actual force trajectories of each of the controllers as well as the corresponding force tracking errors when following a slow reference trajectory of 0.5 Hz. As seen in the figure, the force tracking errors for this reference trajectory are $\pm 10\%$ for the SPR controller, $\pm 2.5\%$ for the TTC controller, and less than $\pm 2\%$ for the TTCA controller. Note that, for this slow reference trajectory, the inner loop velocity controller provides almost exact tracking (steady-state velocity errors less than $\pm 5\%$). However, the force tracking errors of the SPR controller are still four times larger than those of the TTC and TTCA controllers. This is consistent with the theoretical results presented in Section IV. Fig. 7 shows the relative force errors of the three controllers at six different reference trajectory frequencies from 0.5 to 3.0 Hz. We see from the figure that while the force tracking errors for the SPR controller progressively increase from $\pm 10\%$ at a 0.5-Hz reference to $\pm 45\%$ at a 3.0-Hz reference, the corresponding force tracking errors for the TTC and TTCA controllers vary from $\pm 2.5\%$ (at 0.5 Hz) to $\pm 10\%$ (at 3.0 Hz). We conclude that the TTC and TTCA controllers, which incorporate a feedfoward term, significantly outperform the SPR controller over a wide range of reference inputs.

D. Effect of Varying Force Gain k_f

To study the effect of the force gain k_f on the steady-state force tracking errors, the fixed TTC controller was made to follow a 2-Hz sinusoidal force trajectory at varying force gain (k_f) values of 0.1, 0.2, 0.3, 0.4, and 0.5. At this high frequency, the inner loop velocity errors are significant and cannot be ignored. Fig. 8(a) shows the steady-state inner loop velocity references and Fig. 8(b) shows the steady-state inner loop velocity errors for these five values of force gain. As seen, the velocity references and errors are bounded and have almost identical values for the different values of k_f. The velocity reference varies between ± 0.035 m/s and the maximum velocity error is $\pm 17\%$ for each value of k_f. However, Fig. 8(c) shows that the steady-state force errors progressively decrease with increasing values of k_f. Fig. 9 plots $1/k_f$ times velocity error and the force error for each of the five values of k_f. As predicted by the theory of Section IV, the steady-state force tracking error is bounded by $1/k_f$ times the steady-state value of velocity error and as k_f increases, the steady-state force tracking error gets progressively smaller. This verifies the high gain result presented in Section IV.

E. Effect of Adaptive Gain α

To study the effect of the adaptive gain α on the force trajectory tracking performance of the adaptive controller TTCA, the robot was made to follow a 0.25-Hz sinusoidal force trajectory at a low force gain (k_f) of 0.075 at four different adaptive gain (α) values of 0.5, 1.0, 5.0, and 10.0. Fig. 10 shows the evolution over time of the compliance estimate $\hat{\gamma}$ with varying α. As seen, as the value of α increases, the bound on the initial transient in the compliance estimate $\hat{\gamma}$ gets larger while the time required for $\hat{\gamma}$ to converge to its steady-state value decreases. The steady-state value of the $\hat{\gamma}$, however, remains the same despite this fourfold increase in the adaptive gain value α. Similarly, Fig. 11 shows that the upper bounds on steady-state force

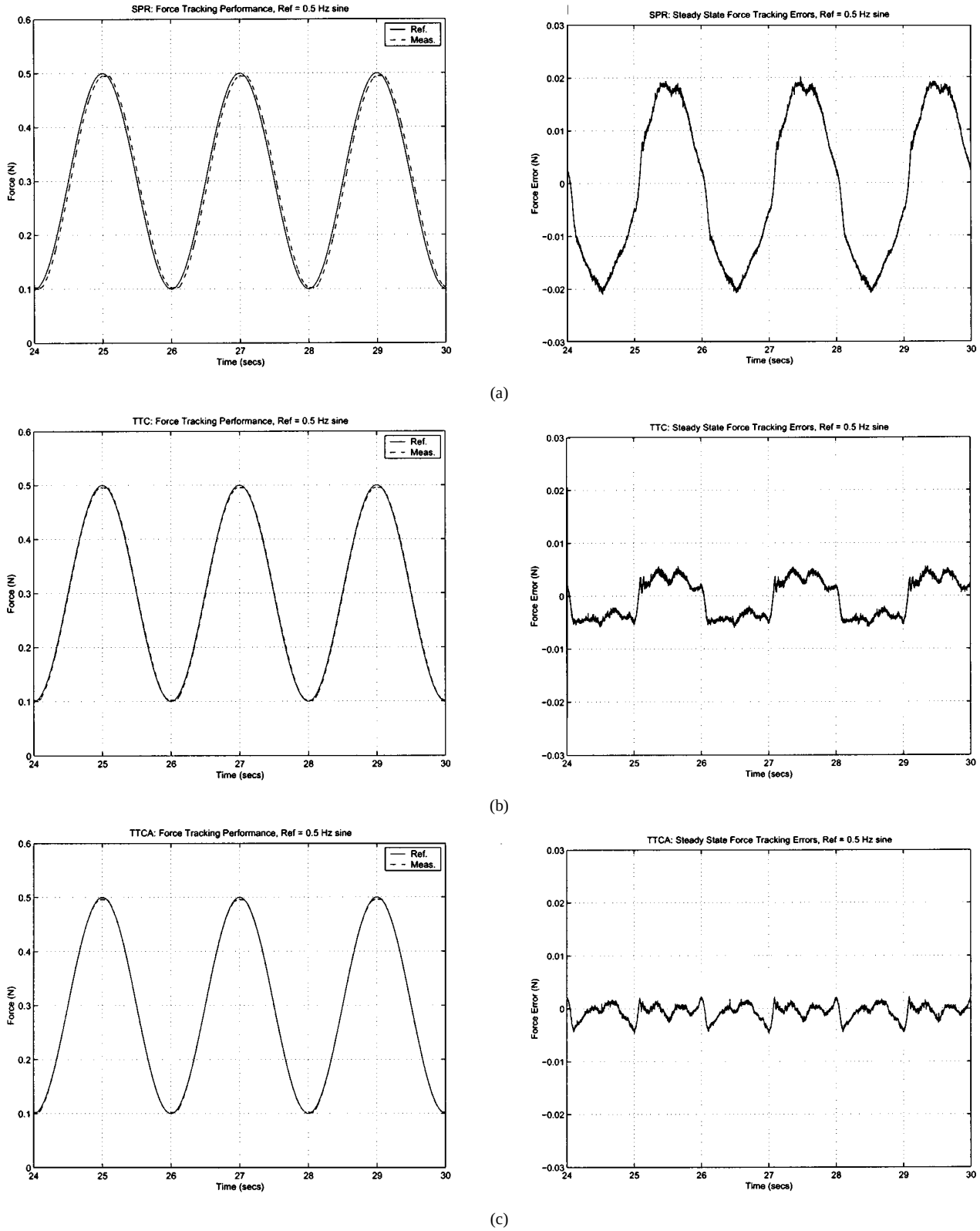

Fig. 6. Trajectory tracking performance of three implicit force controllers: Shown are the force tracking performances of the (a) SPR, (b) TTC, and (c) TTCA controllers when tracking a 0.5 Hz sinusoidal force reference. Left: reference and actual force trajectories; right: force traking error versus time.

tracking errors remain almost identical for all the four values of α. Thus we conclude that the adaptive gain α only affects the transient behavior of the compliance estimate $\hat{\gamma}$ but has no effect on the steady-state force tracking errors of the adaptive TTCA controller.

F. Effect of Reference Trajectory Frequency on Compliance Estimate $\hat{\gamma}$

Fig. 12 shows the behavior of the steady-state value of the compliance estimate $\hat{\gamma}$ with varying reference frequencies. It

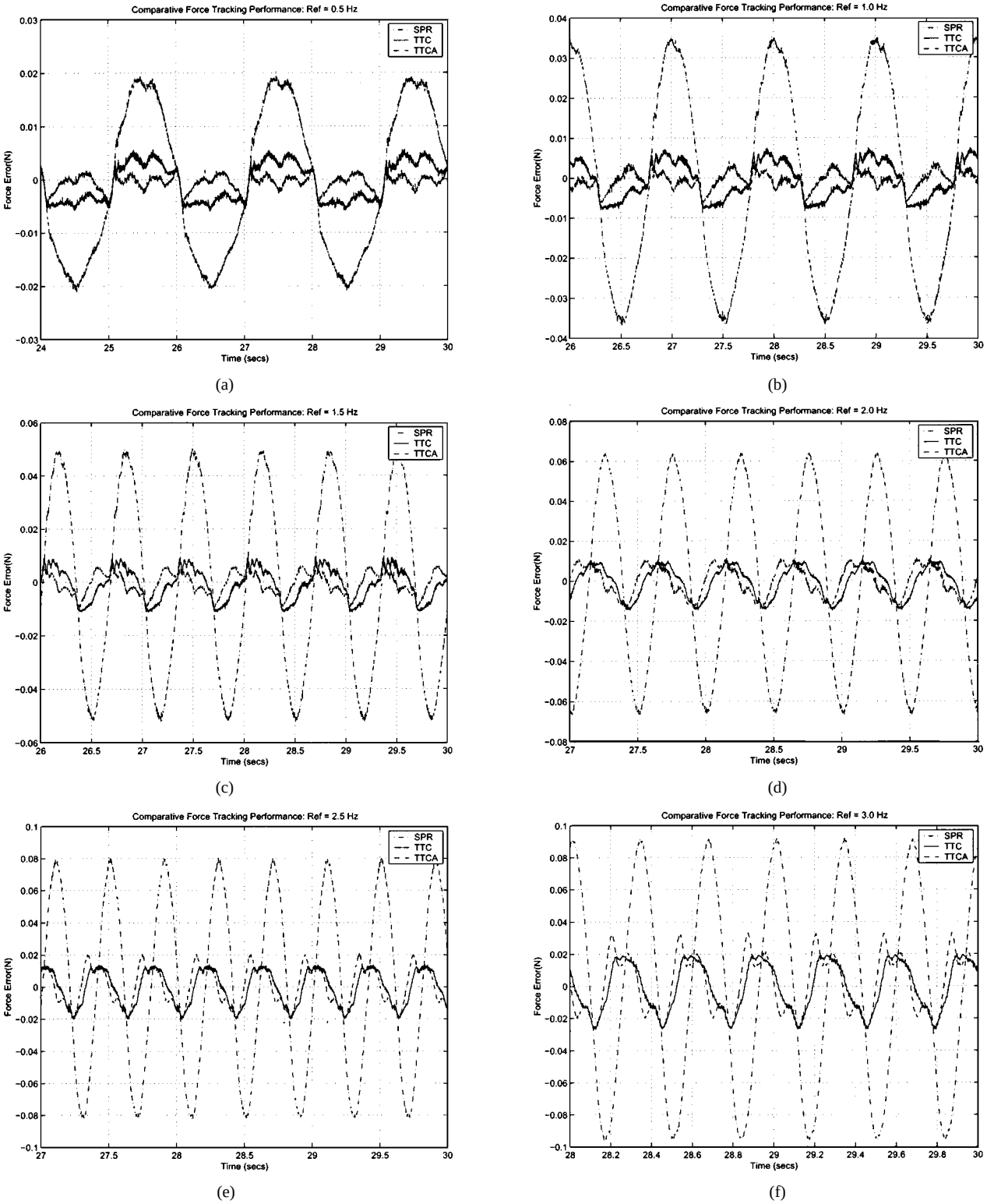

Fig. 7. Comparative force tracking errors of the SPR, TTC, and TTCA controllers at 6 different reference force frequencies. Reference frequency is: (a) 0.5 Hz, (b) 1.0 Hz, (c) 1.5 Hz, (d) 2.0 Hz, (e) 2.5 Hz, and (f) 3.0 Hz. Reference force $f_d(t) = 0.3 + 0.2\sin(2\pi ft)$.

is observed that $\hat{\gamma}$ converges to slightly different values at different reference frequencies. This theoretically unexplained fact can perhaps be explained by the fact that, at lower reference frequencies, unmodeled friction (and stiction) effects are more significant than at higher reference frequencies. The nature of the adaptive update law is such that it compensates, in part, for these friction effects. Hence, at lower frequencies, the compliance estimates converge to values that are slightly higher than the measured compliance of the environment. Further, it is also observed that the steady-state $\hat{\gamma}$ values exhibit higher oscillations at higher frequencies. This effect can be perhaps be explained by the fact the inner loop velocity errors of the simple

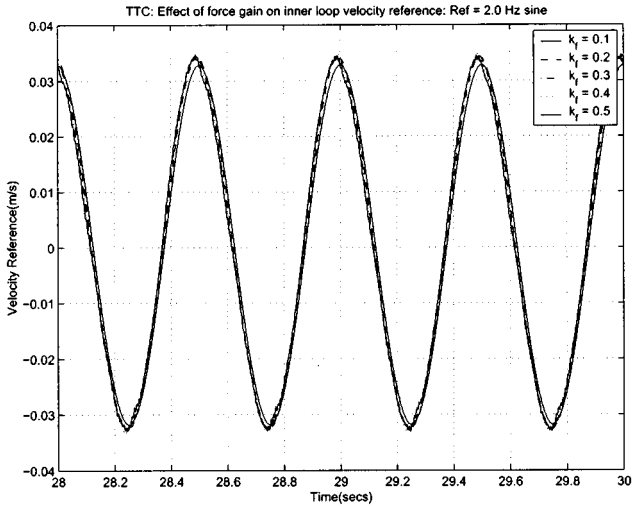

(a)

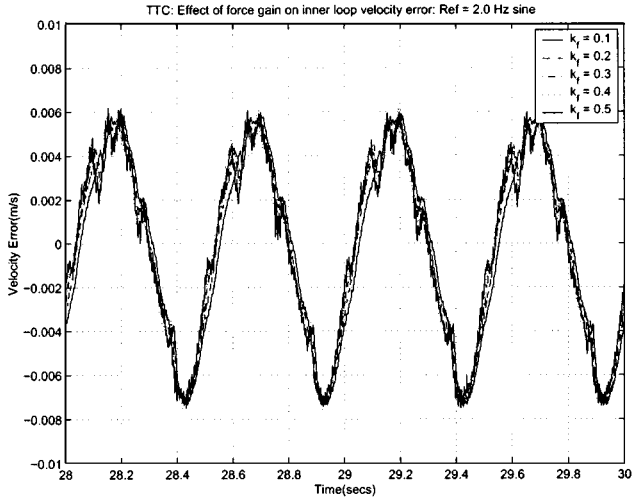

(b)

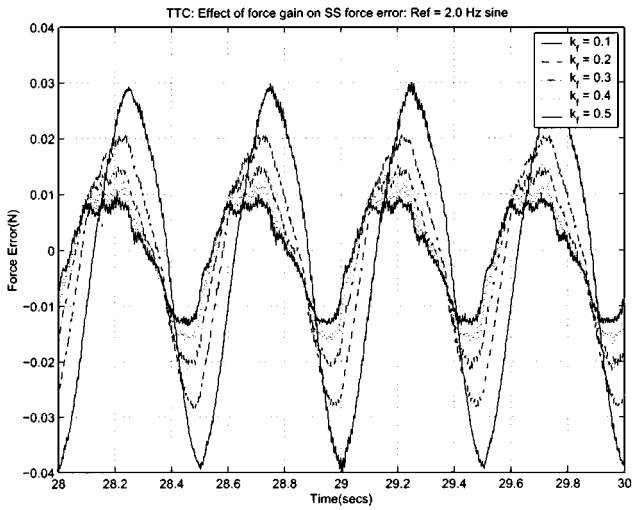

(c)

Fig. 8. TTC: effect of force gain (k_f) on: (a) inner loop velocity reference, (b) inner Loop velocity errors, and (c) force tracking errors. Shown are the responses to a 2-Hz sinusoidal force reference at force gains (k_f) of 0.1, 0.2, 0.3, 0.4, and 0.5.

proportional controller are higher at higher reference frequencies which leads to higher force errors Δf. Further, the magnitude and oscillation frequency of the $\dot{f}_d$ is also higher at higher frequencies. Since $\dot{\hat{\gamma}}$ depends on both Δf and $\dot{f}_d, \hat{\gamma}$ exhibits larger oscillations are higher reference trajectory frequencies.

G. Adaptive (TTCA) Versus Fixed (TTC) Controllers

We have seen in Section V-C that the fixed TTC and the adaptive TTCA controllers provide nearly identical performance with respect to steady-state force tracking errors over a large range of reference frequencies. This, off-course, is to be theoretically expected because in the presence of a suitable reference trajectory (or more precisely, a persistently exciting reference trajectory), the compliance estimate $\hat{\gamma}$ will converge to the actual value of the compliance γ and in the steady-state limit, both the controllers will be identical. In the experiments described in Section V-C, the value of γ used in the fixed TTC controller was exactly experimentally determined. What happens if a wrong value of γ is used in the fixed controller? Fig. 13 shows the force tracking errors of the fixed TTC controller for a 1.0-Hz reference when a value of 0.006 25 m/N is used for γ in place of the correct value of 0.0115 m/N. The steady-state force tracking errors are seen to be more than two times larger than when the correct value is used. The adaptive version suffers from no such handicap since the steady-state values of the compliance estimate are insensitive to initial estimates of the compliance. Thus, we conclude that in the absence of a precise knowledge of the environment compliance or when the environment compliance is liable to change over time, the adaptive controller provides superior force tracking performance.

Another curious fact seen from Fig. 7 is that at low frequencies the fixed TTC controller (using a correct value of γ) provides marginally higher steady-state errors than the adaptive TTCA controller while this behavior is reversed at at higher frequencies. What is the reason for the marginally anomalous behavior? At low frequencies, the inner loop controller provides almost exact trajectory tracking in the absence of friction effects. However, these friction effects are in reality present and lead to steady-state velocity errors which in turn lead to steady-state force tracking errors. The nature of the update law in the adaptive controller TTCA is such that it in part compensates for some of these unmodeled friction effects and $\hat{\gamma}$ converges to a value slightly different from the correct value of γ. This in turn leads to marginally lower steady-state errors at low frequencies. At higher reference frequencies, the velocity errors are no longer negligible and the bounded velocity error model is applicable. As seen in the Section V.F, the compliance estimate exhibits relatively large oscillations at high frequencies and this amounts to a nonzero bounded steady-state value in the compliance estimate error $\tilde{\gamma}$. As seen in Section IV, this adds to upper bound on the steady-state force error for the TTCA controller and hence we get marginally higher steady-state force tracking errors.

H. Force Measurement Delays, Bandwidth Constraints, and Contact Transition Issues

It is well known that the performance of force controllers may sometimes be limited by closed-loop bandwidth constraints and, in extreme cases, by force measurement/processing delays. How

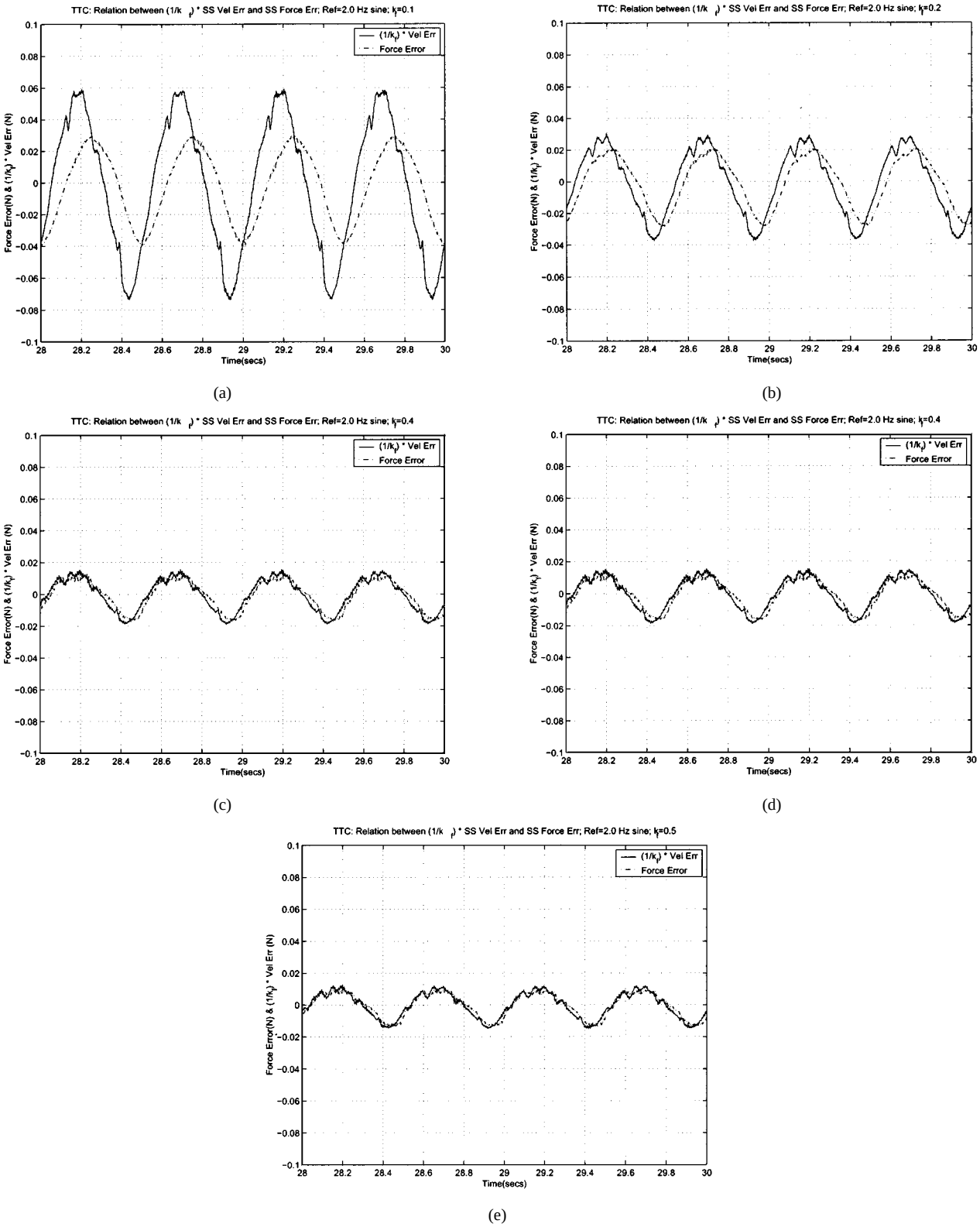

Fig. 9. TTC: effect of bounded velocity errors on steady state force errors. Shown are plots for force gains of (a) 0.1, (b) 0.2, (c) 0.3, (d) 0.4, and (e) 0.5.

did these affect the results of our experiments? In all the experiments reported in this section, both the inner velocity and outer force control loops were implemented in DOS on a 500-MHz Pentium II computer at a real time servo rate of 1 kHz. The latency between a force measurement and the corresponding commanded actuator output was less than 1 ms, whereas the measured closed loop position bandwidth of the robot was 20 Hz. As noted earlier in this section, the frequencies of force reference trajectories varied from 0.5 Hz to 3 Hz, well below the closed-loop system bandwidth. At these reference frequencies, we did not observe any effects of bandwidth limitations on the performance of the three implicit force controllers. It is, of

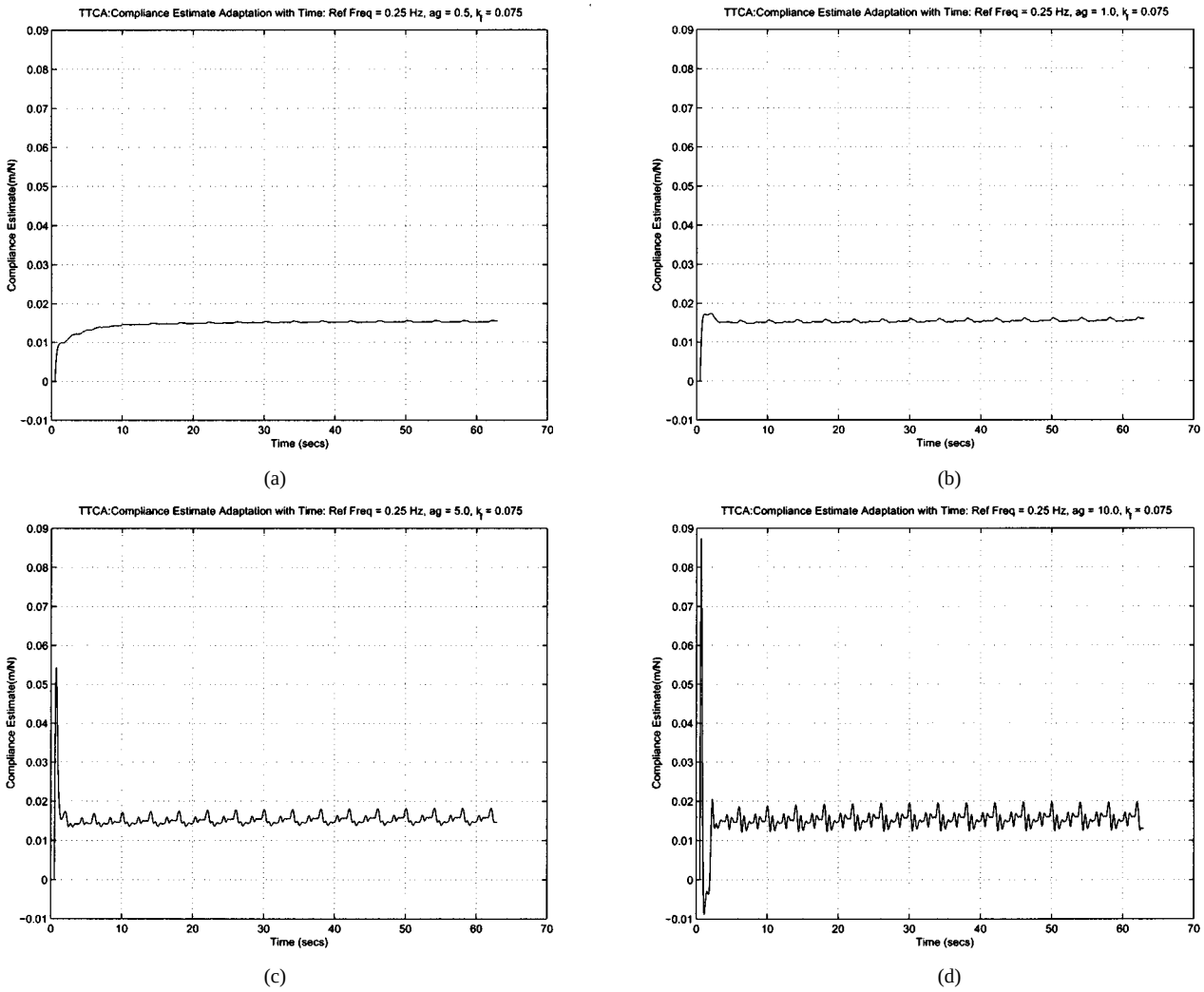

Fig. 10. Effect of varying adaptive gain α on compliance estimate $\hat{\gamma}$. (a) $\alpha = 0.5$. (b) $\alpha = 1.0$. (c) $\alpha = 5.0$. (d) $\alpha = 10.0$.

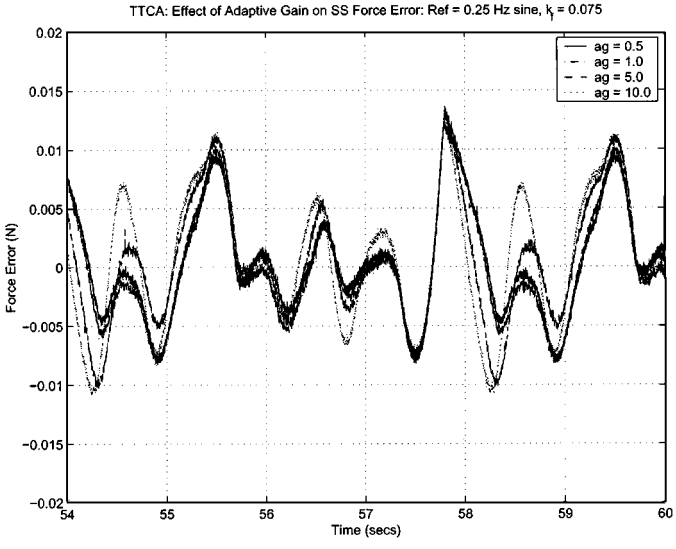

Fig. 11. TTCA: steady-state force tracking errors while following a 0.25-Hz sinusoidal reference at adaptive gains of 0.5, 1.0, 5.0, 10.0. Force gain $k_f = 0.075$.

course, possible to degrade either the servo rate or the closed loop system bandwidth to the point where these effects become noticeable. However, since the primary goal of our study was to study the comparative behavior of the three force control algorithms and the effects of various gain parameters on their performance, we performed our experiments at the high servo rate of 1 kHz.

In all the experiments reported in this paper, all three controllers were in contact with the environment before the desired force trajectory was commanded and remained in contact thereafter. This is consistent with assumption 2 in Section II-A. How do the three controllers compare in their behavior while transitioning from noncontact state to contact state? As noted in [12], the SPR controller is mode-less in its transition. It automatically switches from proportional-velocity control (where the desired tool tip velocity is proportional to the desired force), when the robot is not in contact with the environment, to force regulation mode when contact is made with the environment. The transition properties of the TTC and TTCA controllers are not as well behaved. However, it is our experience that an *ad hoc* mode switching, consisting of turning off the feedforward term when the robot is not in contact with the environment and switching it on once contact is detected (through an increase in the sensed force above a small threshold) works satisfactorily in practice. This results in the robot remaining in stable proportional-ve-

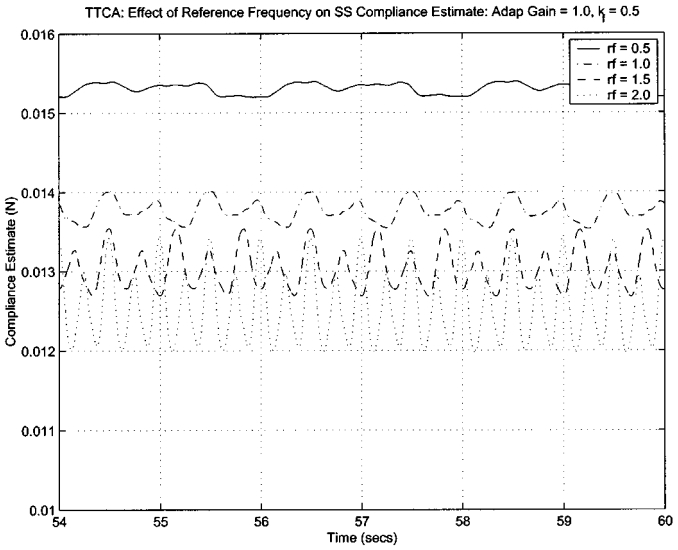

Fig. 12. Steady-state compliance estimate ($\hat{\gamma}$) values at four different reference trajectory frequencies.

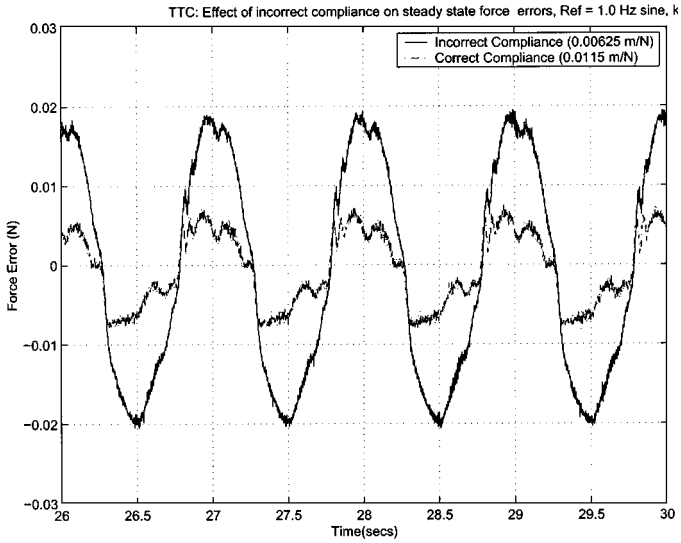

Fig. 13. Force tracking errors of the TTC controller: the effect of using incorrect environment compliance estimates. Force reference frequency $= 1.0$ Hz.

locity control mode when not in contact and in stable force control mode when it was in contact with the environment.

VI. Conclusion

In this paper we reviewed one previously reported and presented two new position/velocity based implicit force controllers. Detailed results, presented in Sections IV and V, are only summarized here.

1) We present a new adaptive force control algorithm for position/velocity controlled robot arms in contact with surfaces of unknown linear compliance. This controller, as well as its nonadaptive counterpart, provably guarantees global asymptotic convergence of force trajectory tracking errors to zero when the robot is under exact or asymptotically exact inner loop velocity control. To the best of our knowledge, this is the first reported proof of global asymptotic stability in force trajectory tracking for this class of position/velocity based controllers.
2) We report an additional high gain result for the new fixed (nonadaptive) controller which guarantees arbitrarily small force tracking errors in the presence of bounded inner loop velocity tracking errors.
3) We report an extensive comparative experimental study which corroborates the theory presented in the paper and shows the performance of the new adaptive controller as well as its nonadaptive counterpart to be superior to the previously reported position based integral force controller.

Acknowledgment

The authors would like to thank Dr. E. deJuan, Dr. P. Jensen, A. Barnes, T. Shelly, P. Gupta, and other members of The Johns Hopkins University MADLAB for their time and invaluable help with resources and equipment. They would also like to thank Dr. R. Taylor, Dr. P. Berkelman, and Dr. R. Kumar of The Johns Hopkins University ERC in Computer Assisted Surgery for their help during various parts of the project, and Dr. W. Rugh of the Department of Electrical and Computer Engineering at the Johns Hopkins University for elucidating even the most arcane systems theory results with clarity and grace.

References

[1] T. Yoshikawa, "Force control of robot manipulators," in *Proc. IEEE Int. Conf. Robotics and Automation*, vol. 1, 2000, pp. 220–226.
[2] N. Hogan, "Impedence control: An approach to manipulation: Part I—Theory," *J. Dynamic Syst., Measurement Contr.*, vol. 107, pp. 1–7, Mar. 1985.
[3] ——, "Impedence control: An approach to manipulation: Part II—Implementation," *J. Dynamic Syst., Measurement Contr.*, vol. 107, pp. 8–16, Mar. 1985.
[4] ——, "Impedence control: An approach to manipulation: Part III—Applications," *J. Dynamic Syst., Measurement Contr.*, vol. 107, pp. 17–24, Mar. 1985.
[5] M. Raibert and J. Craig, "Hybrid position/force control of manipulators," *J. Dynamic Syst., Measurement Contr.*, vol. 103, no. 2, pp. 126–133, Feb. 1981.
[6] M. Mason, "Compliance and force control for computer controlled manipulators," *IEEE Trans. Syst., Man, Cybern.*, vol. SMC-11, pp. 418–432, June 1981.
[7] T. Yoshikawa, "Dynamic hybrid position/force control of robot manipulators—Description of hand constraints and calculation of joint driving force," *IEEE J. Robot. Automat.*, vol. RA-3, pp. 386–392, Oct. 1987.
[8] N. McClamroch and D. Wang, "Feedback stabilization and tracking of constrained robots," *IEEE Trans. Automat.Contr.*, vol. 33, pp. 419–426, May 1988.
[9] B. Siciliano and L. Villani, "A passivity-based approach to force regulation and motion control of robot manipulators," *Automatica*, vol. 32, no. 3, pp. 443–447, Mar. 1996.
[10] R. Kankaanranta and H. Koivo, "Dynamics and simulation of compliant motion of a manipulator," *IEEE J. Robot. Automat.*, vol. 4, pp. 163–173, Apr. 1988.
[11] L. Villani, C. C. de Wit, and B. Brogliato, "An exponentially stable adaptive control for force and position tracking of robot manipulators," *IEEE Trans. Automat.Contr.*, vol. 44, pp. 778–802, Apr. 1999.
[12] J. De Schutter and H. Van Brussel, "Compliant robot motion II. A control approach based on external control loops," *Int. J. Robot. Res.*, vol. 7, no. 4, pp. 18–33, Aug. 1988.
[13] R. Volpe and P. Khosla, "A theoretical and experimental investigation of explicit force control strategies for manipulators," *IEEE Trans. Automat.Contr.*, vol. 38, pp. 1634–1650, Nov. 1993.

[14] S. D. Eppinger and W. P. Seering, "Three dynamic problems in robot force control," *IEEE Trans. Robot. Automat.*, vol. 8, pp. 751–758, Dec. 1992.
[15] G. Alici and R. W. Daniel, "Development and experimental verification of a mathematical model for robot force control design," in *IEEE/RSJ Int. Conf. Intelligient Robots and Systems*, vol. 2, 1993, pp. 1559–1565.
[16] S. Arimoto, Y. Liu, and T. Naniwa, "Model-based adaptive hybrid control for geometrically constrained robots," in *Proc. IEEE Int. Conf. Robotics and Automation*, 1993, pp. 163–173.
[17] L. L. Whitcomb, S. Arimoto, T. Naniwa, and F. Ozaki, "Adaptive model-based hybrid control of geometrically constrained arms," *IEEE Trans. Robot. Automat.*, vol. 13, pp. 105–116, Feb. 1997.
[18] J. T. Wen and S. Murphy, "Stability analysis of position and force control for robot arms," *IEEE Trans. Automat.Contr.*, vol. 36, pp. 365–371, Mar. 1991.
[19] J. Maples and J. Becker, "Experiments in force control of robotic manipulators," in *Proc. IEEE Int. Conf. Robotics and Automation*, 1986, pp. 695–702.
[20] B. Waibel and E. Kazerooni, "Theory and experiment on the stability of robot compliance control," *IEEE Trans. Robot. Automat.*, vol. 7, pp. 95–104, June 1991.
[21] G. Duellen, H. Münch, and D. Surdilovic, "Automated force control schemes for robotic deburring," in *Proc. IEEE Int. Conf. Industrial Electronics, Control and Automation*, 1992, pp. 912–917.
[22] G. Alici and R. W. Daniel, "Static friction effects during hard-on-hard contact tasks and thier implications for manipulator design," *Int. J. Robot. Res.*, vol. 13, no. 6, pp. 508–520, Dec. 1994.
[23] D. Surdilovic and J. Kirchoff, "A new position based force/impedence control for industrial robots," in *Proc. IEEE Int. Conf. Robotics and Automation*, 1996, pp. 629–634.
[24] D. Surdilovic, "Contact stability issues in position based impedence control: Theory and experiments," in *Proc. IEEE Int. Conf. Robotics and Automation*, 1996, pp. 1675–1680.
[25] P. Rocco, G. Ferretti, and G. Magnani, "Implicit force control for industrial robots in contact with stiff surfaces," *Automatica*, vol. 33, no. 11, pp. 2041–2047, Nov. 1997.
[26] G. Ferretti, G. Magnani, and P. Rocco, "Impedence control for industrial robots," in *Proc. IEEE Int. Conf. Robotics and Automation*, 2000, pp. 4028–4033.
[27] ——, "Toward the impelementation of hybrid position/force control in industrial robots," *IEEE Trans. Robot. Automat.*, vol. 13, pp. 838–845, Dec. 1997.
[28] D. W. Robinson and G. A. Pratt, "Force controllabe hydro-elastic actuator," in *Proc. IEEE Int. Conf. Robotics and Automation*, 2000, pp. 1321–1327.
[29] N. Sadegh and R. Horowitz, "Stability and robustness analysis of a class of adaptive conrollers for robot arms," *Int. J. Robot. Res.*, vol. 9, pp. 74–92, June 1990.
[30] L. L. Whitcomb, A. Rizzi, and D. E. Koditschek, "Comparative experiments with a new adaptive controller for robot arms," *IEEE Trans. Robot. Automat.*, vol. 9, pp. 59–70, Feb. 1993.
[31] W. J. Rugh, *Linear System Theory*, 2nd ed. Upper Saddle River, NJ: Prentice-Hall, 1996.
[32] H. K. Khalil, *Nonlinear Systems*, 1st ed. New York: Maxmillan, 1992.
[33] M. Vidyasagar, *Nonlinear Systems Analysis*, 2nd ed. Englewood Cliffs, NJ: Prentice-Hall, 1993.
[34] R. Kumar, P. Berkelman, P. Gupta, A. Barnes, P. S. Jensen, L. L. Whitcomb, and R. H. Taylor, "Preliminary experiments in cooperative human/robot force control for robot assisted microsurgical manipulation," in *Proc. IEEE Int. Conf. Robotics and Automation*, vol. 1, 2000, pp. 610–617.
[35] R. H. Taylor, P. Jensen, L. L. Whitcomb, A. Barnes, R. Kumar, D. Stoianovici, P. Gupta, Z. Wang, E. de Juan, and L. R. Kavoussi, "A steady-hand robotic system for microsurgical augmentation," *Int. J. Robot. Res.*, vol. 18, no. 12, pp. 1201–1210, Dec. 1999.
[36] D. Stoianovici, L. L. Whitcomb, J. H. Anderson, R. H. Taylor, and L. R. Kavoussi, "A modular surgical system for image guided percutaneous procedures," in *Lecture Notes in Computer Science 1496: Medical Imaging and Computer-Assisted Intervention—MICCAI'98*, W. M. Wells, A. Colchester, and S. Delp, Eds, Berlin, Germany: Springer-Verlag, Oct. 1998, vol. 1496, pp. 404–410.

Jaydeep Roy (M'97) received the B.Tech. degree in mechanical engineering from the Indian Institute of Technology (IIT), Bombay, India, in 1994 and the M.S. and Ph.D. degrees in mechanical engineering from the Johns Hopkins University, Baltimore, MD, in 1997 and 2001, respectively.

From August 1994 to July 1995, he was employed as a Research Engineer in the Robotics Laboratory at IIT Bombay. He is currently a Post-Doctoral Fellow at the Johns Hopkins University, holding joint appointments in the Department of Mechanical Engineering and the Department of Otolaryngology (Head and Neck Surgery). His research interests include the design, analysis, and control of industrial and surgical robotic systems.

Louis L. Whitcomb (S'87–M'87) received the B.S. and Ph.D. degrees from Yale University, New Haven, CT, in 1984 and 1992, respectively.

His research focuses on the dynamics and control of mechanical things. He is an Associate Professor of Mechanical Engineering at the Johns Hopkins University, Baltimore, MD.